Characterization of CaO–TiO$_2$ and V$_2$O$_5$/CaO–TiO$_2$ catalysts and their activity for cyclohexanol conversion

Benjaram M. Reddy [*], K. Jeeva Ratnam, Pranjal Saikia

Inorganic and Physical Chemistry Division, Indian Institute of Chemical Technology, Hyderabad 500 007, India

Abstract

Influence of CaO on TiO$_2$ (anatase) phase stabilization and dispersion behaviour of V$_2$O$_5$ over CaO–TiO$_2$ mixed oxide support have been investigated using XRD, FTIR, Raman, XPS, and BET surface area techniques. The CaO–TiO$_2$ binary oxide (1:1 molar ratio) was synthesized by a homogeneous co-precipitation method from ultrahigh dilute solutions of the corresponding chlorides and calcined at various temperatures from 723 to 1273 K. On the calcined CaO–TiO$_2$ support (723 K) various amounts of V$_2$O$_5$ (2.5–10 wt.%) were deposited from ammonium metavanadate by a wet impregnation method and calcined at different temperatures. Conversion of cyclohexanol to cyclohexanone/cyclohexene was performed as a model reaction to assess the acid–base properties of the prepared catalysts. The CaO–TiO$_2$ composite oxide exhibits reasonably high specific surface area and high thermal stability up to 1273 K retaining titania-anatase phase. The deposited V$_2$O$_5$ over CaO–TiO$_2$ support is present mostly in a dispersed form. Further, a strong and preferential interaction between the basic CaO and the dispersed V$_2$O$_5$ leads to the formation of CaVO$_3$ and the physicochemical properties of the prepared catalysts are clearly reflected in their catalytic activity.
© 2006 Elsevier B.V. All rights reserved.

Keywords: CaO–TiO$_2$; TiO$_2$-anatase; Vanadium oxide; CaVO$_3$; Mixed oxides; Dispersion; Basic oxide; Cyclohexanol; Cyclohexanone; Cyclohexene

1. Introduction

Bulk V$_2$O$_5$ cannot be used as a catalyst in industrial processes because of its poor thermal stability and mechanical strength leading to fast deactivation of the catalyst. Moreover, it is a known fact that bulk V$_2$O$_5$ leads to high combustion of organic molecules to carbon oxides at high temperatures. Being free from these demerits, supported vanadium oxide catalysts have emerged as an important model system in heterogeneous oxidation catalysis [1–5]. Thus supported V$_2$O$_5$ systems have been employed in partial oxidation of *o*-xylene to phthalic anhydride [6], ammoxidation of aromatic compounds [7,8], selective catalytic reduction (SCR) of nitrogen oxides [9–11], oxidation of SO$_2$ to SO$_3$ [12,13], oxidative dehydration of alkanes [14,15], and so on. Depending on the nature of the reaction to be catalysed, supports for V$_2$O$_5$ have been varied as most of the studies dealt with characterization of vanadium oxide

species on various supports reveal that the activity and selectivity of the catalyst is highly sensitive to the nature of the support employed [1,2,16–18]. The physicochemical nature of the support contributes to the metal dispersion and electronic effects, respectively, besides rendering high surface area and better thermal stability [19,20]. Different forms of dispersed vanadium oxide have been identified for different loadings. When the loading is low (<5%), vanadium oxide will be in a highly dispersed state and forms isolated tetrahedral vanadate species. Increase of loading normally leads to polymeric two-dimensional networks in distorted tetrahedral and square pyramidal coordination. At high loadings, three-dimensional V$_2$O$_5$ crystallites in octahedral coordination are generally reported [21].

Titania has gained widespread significance as catalyst as well as support due to its marvellous promotional effect, which is the consequence of its strong redox characteristics [1,2,22,23]. The TiO$_2$-anatase has been exploited for several photo catalytic reactions for elimination of organic pollutants from waste-waters [23], hydrolysis of HCN and COS, and epoxidation of olefins [24]. In case of V$_2$O$_5$/TiO$_2$ catalysts, the dispersed vanadium oxide is very sensitive to the phase of the support [18]. Among the three structural polymorphs of TiO$_2$, namely anatase, rutile

* Corresponding author. Tel.: +91 40 2716 0123; fax: +91 40 2716 0921.
E-mail addresses: bmreddy@iict.res.in, mreddyb@yahoo.com
(B.M. Reddy).

and brookite, anatase is the most preferred phase and is widely studied [9,25–32]. Literature clearly reveals that the activity per gram of V_2O_5/TiO_2 catalyst increases with increase of vanadia loading up to the theoretical monolayer coverage of the support ($\sim$0.1 wt.% m^{-2}) [1]. Unfortunately, TiO_2-anatase bears major drawbacks like low specific surface area and low thermal stability of the active anatase phase at high temperatures. The loss in activity normally occurs due to sintering and subsequent phase transformation from anatase to thermodynamically stable rutile form. Therefore, there are several attempts in the literature to obtain titania-based systems combined with another stable oxide to design improved catalysts for various applications [33–36].

Various basic oxides such as MgO, CaO, and Ga_2O_3 with various promoters have been quite extensively investigated due to their high activity and selectivity for oxidative coupling of methane [37–39]. Both surface acid–base characteristics and redox properties of the catalysts influence selective oxidation or oxidative dehydrogenation of alkanes [40,41]. In certain cases, basic oxide supported vanadium oxide was reported to show better performance than acidic oxide supported ones [42]. An increase in the basicity of the catalyst enhances the selectivity towards oxygenates [43,44]. For example, $V_2O_5/Ga_2O_3–TiO_2$ and $V_2O_5/La_2O_3–TiO_2$ combination catalysts possessing both acid–base and redox properties together were found to exhibit better catalytic properties for selective oxidation of 4-methylanisole to anisaldehyde and synthesis of 2,6-dimethylphenol from methanol and cyclohexanone, respectively [43,44]. In view of the significance of mixed oxide supported vanadium oxide catalysts for various commercially important reactions the present investigation was undertaken. In this study a CaO–TiO_2 binary oxide (1:1 ratio) support was synthesised and impregnated with various amount of V_2O_5 and subjected to different calcination temperatures. Physicochemical properties of the prepared samples were investigated by means of XRD, FTIR, Raman spectroscopy, XPS, and BET surface area techniques. To assess the acid–base properties, conversion of cyclohexanol to cyclohexene/cyclohexanone was performed as a model reaction [45], since the competitive dehydration/dehydrogenation reaction of cyclohexanol is considered as a universal test reaction for evaluation of acid–base properties of the solid catalysts [46].

2. Experimental

2.1. Catalyst preparation

The CaO–TiO_2 (1:1 mole ratio based on oxides) was prepared by an aqueous homogeneous co-precipitation method using urea as hydrolyzing agent. The requisite quantities of titanium tetrachloride ($TiCl_4$, Fluka, AR grade) and calcium chloride ($CaCl_2 \cdot 2H_2O$; Loba Chemie, GR grade), dissolved separately in deionised water were mixed together. Cold $TiCl_4$ was first digested in cold concentrated HCl and diluted with deionised water. Solid urea with a metal to urea molar ratio of 1:2.5 was added to the mixer solution and subsequently heated slowly to 363–368 K on a hot plate with vigorous stirring. The pH of the solution was monitored at different intervals of time. A change in pH was observed after the solution had reached 363–368 K

and attained a final value between 7 and 8. Heating was further continued at the same temperature for 6 h more and the pH of the solution increased by adding dilute ammonia in order to get complete precipitation. The resulting precipitates were filtered and washed with deionised water until free from chloride ions. The obtained gel was then oven dried at 383 K for 12 h and calcined at various temperatures from 723 to 1273 K for 6 h in open-air atmosphere.

The calcined CaO–TiO_2 mixed oxide support (723 K) was impregnated with various amounts of V_2O_5 ranging from 2.5 to 10 wt.% by a wet impregnation method with stoichiometric aqueous solution of ammonium metavanadate dissolved in 2 M aqueous oxalic acid solution. The excess water was evaporated on a water-bath under constant stirring. The impregnated samples were oven dried at 383 K for 16 h and calcined at 723 K for 5 h under oxygen flow.

2.2. Catalyst characterization

The BET surface areas of the samples were determined by N_2 physisorption at liquid nitrogen temperature (77 K) on a Micromeritics Gemini 2360 instrument. Degassing of the samples was performed for considerable time under helium flow to ensure no pre-absorbed moisture in the samples. The X-ray diffraction analyses of the samples were carried out on a Siemens D-5000 diffractometer using Cu K$_\alpha$ radiation source and Scintillation counter detector. The XRD phases present in the samples were identified with the help of ASTM Powder Data Files. Fourier transform infrared spectra were recorded on a Nicolet 740 FTIR spectrometer at ambient conditions by using KBr as diluent. Raman spectra were recorded on a Nicolet FT-Raman 960 Spectrometer in the 4000–100 cm^{-1} range at a spectral resolution of 2 cm^{-1} using the 1064 nm exciting line ($\sim$600 mV) of a Nd:YAG laser (Spectra Physics, USA). The XPS spectra were recorded on a VG Scientific Lab 210 spectrometer by using Mg K$_\alpha$ (1253.6 eV) radiation as the excitation source. The binding energies (BE) were referenced to C 1s line at 284.6 eV [47,48]. The finely ground oven dried samples were dusted on a double stick graphite sheet and mounted on the standard sample holder. The sample holder was then transferred into the analysis chamber.

2.3. Catalyst evaluation

The vapour phase conversion of cyclohexanol to cyclohexanone/cyclohexene was investigated in a down flow fixed-bed micro-reactor at different temperatures under normal atmospheric pressure. In a typical experiment ca. 2 g of sample was secured between two plugs of pyrex glass wool inside the glass reactor (pyrex glass tube, o.d. 1 cm and i.d. 0.8 cm) and above the catalyst bed filled with glass chips in order to act as preheating zone. The reactor was placed vertically inside a tubular furnace, which can be heated electrically and connected to a temperature indicator-cum-controller. The catalyst was pre-activated in a flow of air (30 ml min^{-1}) at 723 K for 5 h prior to the reaction. After the activation, the temperature was adjusted to the desired level and cyclohexanol was fed from a motorized syringe

pump (Perfusor Secura FT, Germany) into the vaporizer where it was allowed to mix uniformly with air or nitrogen before entering the preheating zone of the reactor. The liquid products collected through the spiral condensers in the ice cooled freezing traps were analysed by a gas chromatograph with FID and using OV-17 column. The main products obtained were cyclohexene, cyclohexanone, and phenol along with some traces of unidentified products. The activity data was collected under study state conditions. The conversion and selectivity were calculated as per the procedure described elsewhere [44].

3. Result and discussion

The N_2 BET surface areas of CaO–TiO$_2$ and V$_2$O$_5$/CaO–TiO$_2$ samples calcined at various temperatures from 723 to 1273 K are presented in Table 1. The CaO–TiO$_2$ support calcined at 723 K exhibited a BET surface area of 77 m^2 g^{-1}, which decreased to 21 m^2 g^{-1} at 1273 K. A progressive decrease in the surface area with increasing calcination temperature is mainly due to sintering of the samples at higher calcination temperatures [49,50]. With impregnation of V$_2$O$_5$, the active component in this case, surface area of the support tends to decrease as quoted elsewhere due to penetration of the dispersed vanadium oxide species into the micro-pores of the support [1,17,44]. As expected, the surface area of V$_2$O$_5$/CaO–TiO$_2$ samples calcined at 773 K decreased with increase of vanadium oxide loading from 2.5 to 10 wt.%. A close inspection of Table 1 reveals that the decrease in the BET surface area of the 1273 K calcined samples is more in the case of vanadia impregnated samples (78%) in comparison to the pure support (72%). The noted loss in the surface area may be due to a strong interaction between the acidic V$_2$O$_5$ and the basic CaO and narrowing of the pores resulting from the penetration of the dispersed vanadium oxide into the pores of the support [1,51,52].

The X-ray powder diffraction patterns of CaO–TiO$_2$ and 10 wt.% V$_2$O$_5$/CaO–TiO$_2$ samples calcined at various temperatures are shown in Figs. 1 and 2, respectively. The XRD patterns

Table 1
BET surface area of CaO–TiO$_2$ and V$_2$O$_5$/CaO–TiO$_2$ samples calcined at different temperatures

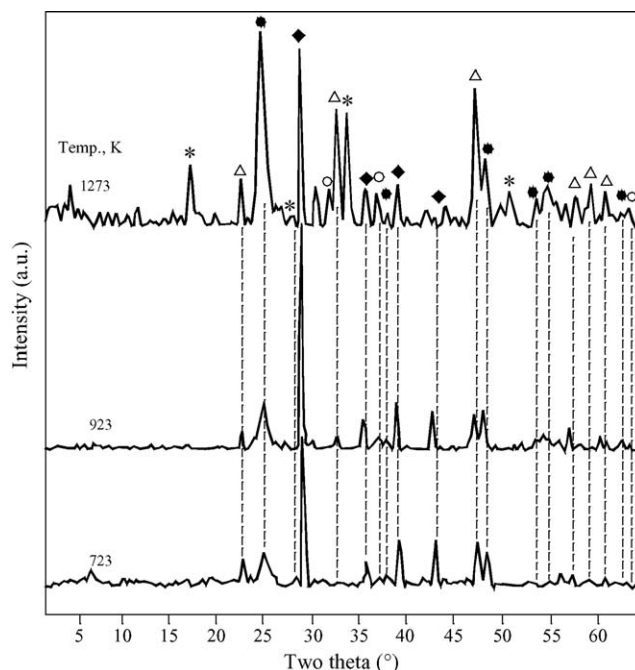| Sample	BET surface area (m^2 g^{-1})
723 K	
CaO–TiO$_2$	77
2.5% V$_2$O$_5$/CaO–TiO$_2$	70
5% V$_2$O$_5$/CaO–TiO$_2$	65
7.5% V$_2$O$_5$/CaO–TiO$_2$	49
10% V$_2$O$_5$/CaO–TiO$_2$	42
923 K	
CaO–TiO$_2$	64
10% V$_2$O$_5$/CaO–TiO$_2$	25
1073 K	
CaO–TiO$_2$	26
10% V$_2$O$_5$/CaO–TiO$_2$	16
1273 K	
CaO–TiO$_2$	21
10% V$_2$O$_5$/CaO–TiO$_2$	9

Fig. 1. X-ray diffraction patterns of CaO–TiO$_2$ sample calcined at different temperatures: (●) peaks due to TiO$_2$-anatase; (*) peaks due to Ca(OH)$_2$; (♦) peaks due to CaCO$_3$; (○) peaks due to CaO; (△) peaks due to CaTiO$_3$.

of the CaO–TiO$_2$ binary oxide calcined at 723 K (Fig. 1) reveal relatively poor crystallinity and amorphous nature of the sample. A bunch of broad diffraction peaks due to titania-anatase phase (JCPDS File No. 21-1272) and CaCO$_3$ (JCPDS File No. 24-27) could be observed. With increase in calcination temperature, the intensity of the characteristic lines due to titania-anatase phase increased. Also new set of peaks are observed which could be attributed to the formation of CaTiO$_3$ phase (JCPDS File No. 22-153). Some characteristic XRD peaks due to CaO (JCPDS File No. 4-777) are also noted. Some additional peaks due to Ca(OH)$_2$ (JCPDS File No. 4-733) are also seen which reveal that the precipitated hydroxides have not been completely dehydroxylated during calcination. Literature reveals that transformation of anatase to rutile is thermodynamically feasible beyond 873 K in impurity free TiO$_2$ samples [22]. Very interestingly, no diffraction lines due to titania-rutile (JCPDS File No. 21-1276) phase are observed even up to the calcination temperature of 1273 K in the present study. Thus the XRD results reveal that the CaO–TiO$_2$ mixed oxide contains mainly anatase phase and at high temperatures some portions of this mixed oxide is converted into CaTiO$_3$ and is thermally quite stable up to 1273 K. In case of V$_2$O$_5$/CaO–TiO$_2$ sample also (Fig. 2), as calcination temperature increased up to 1073 K, the intensity of the lines due to titania-anatase phase increased. At 1273 K, a total transformation of titania-anatase into rutile phase and formation of CaTiO$_3$ and CaVO$_3$ (JCPDS File No. 14-127) compounds are observed. The formation of CaTiO$_3$ is more prominent while the lines due to CaVO$_3$ are less in intensity and both the phases observed only at higher temperatures. The presence of XRD lines due to CaCO$_3$ up to 923 K indicates that it has not been totally decomposed into CaO during calcination. In this case
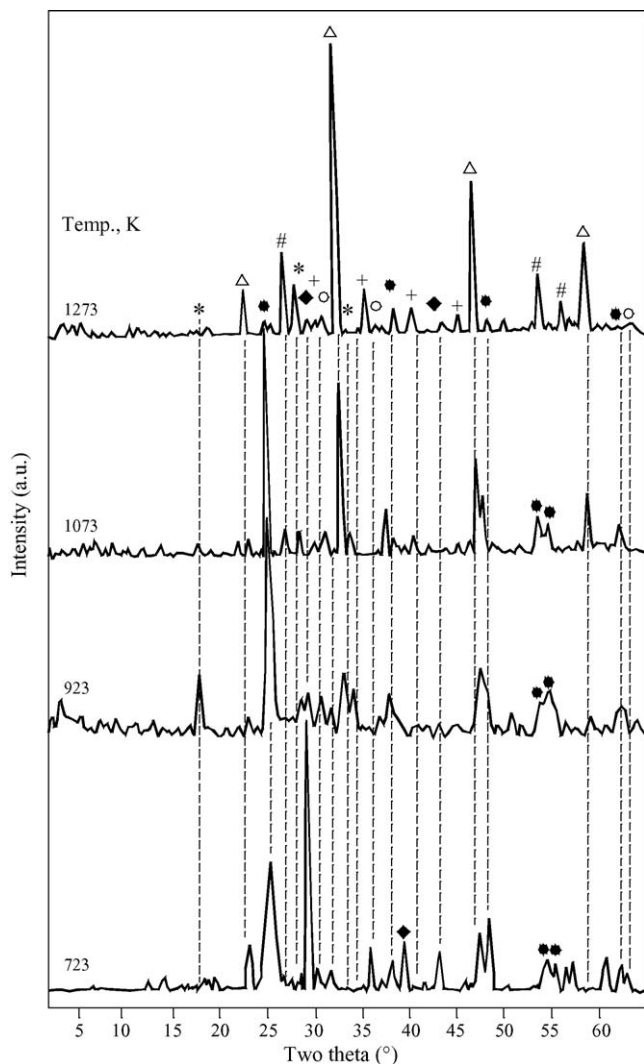
Fig. 2. X-ray diffraction patterns of 10 wt.% V_2O_5/CaO–TiO$_2$ sample calcined at different temperatures: (●) peaks due to TiO$_2$-anatase; (*) peaks due to Ca(OH)$_2$; (♦) peaks due to CaCO$_3$; (#) peaks due to TiO$_2$-rutile; (○) peaks due to CaO; (△) peaks due to CaTiO$_3$; (+) peaks due to CaVO$_3$.

also, characteristics peaks due to Ca(OH)$_2$ which is formed in the preparation stage, is noted. Absence of XRD lines due to crystalline vanadia phase implies that the impregnated V_2O_5 is in a highly dispersed or amorphous state over the support. A close inspection of Figs. 1 and 2 reveals that calcination temperature as well as the vanadia content are equally important for the transformation of TiO$_2$ and CaO into their corresponding thermodynamically stable oxide forms.

FTIR spectra of CaO–TiO$_2$ sample calcined at various temperatures revealed the presence of two prominent peaks at 870 and $\sim$720 cm^{-1} which are the characteristic absorption bands of Ca–O [53]. As the calcination temperature increased the intensity of these two peaks decreased drastically. At 1073 K and above, complete disappearance of the Ca–O characteristics peaks and appearance of new bands due to the formation of CaTiO$_3$ phase in the region 400–600 cm^{-1} are noticed. The two peaks at $\sim$575 and $\sim$455 cm^{-1} are the representative peaks of CaTiO$_3$, where the former peak is due to Ti–O stretch and
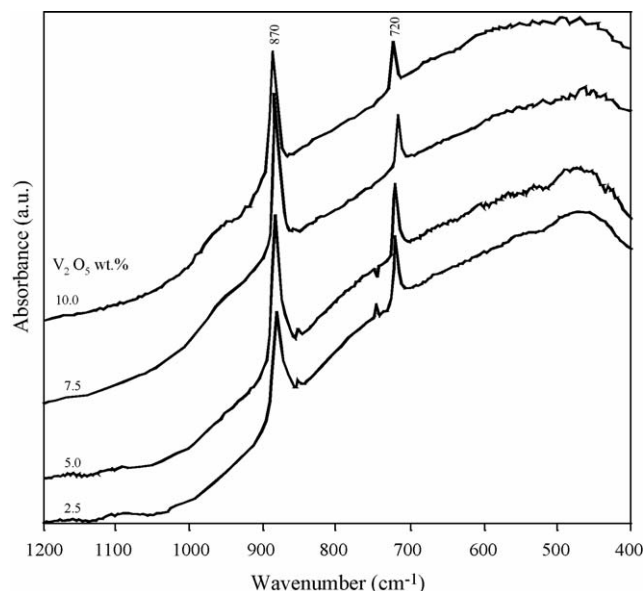

Fig. 3. FTIR spectra of V_2O_5/CaO–TiO$_2$ samples containing various amounts of V_2O_5 and calcined at 723 K.

the later to Ti–O$_3$ torsion, respectively [54]. Representative FTIR spectra of V_2O_5/CaO–TiO$_2$ samples containing various amounts of V_2O_5 and calcined at 723 K are shown in Fig. 3. The spectra reveal the presence of two prominent peaks at 870 and $\sim$720 cm^{-1} as observed in the case of pure support which are the characteristic absorption bands of Ca–O [53]. According to literature reports the IR spectrum of pure V_2O_5 gives sharp bands at 1020 and 825 cm^{-1} due to V=O stretching and V–O–V deformation modes, respectively [1]. It is also an established fact that V_2O_5 forms a layer structure on TiO$_2$ (anatase) with the expose of the (0 1 0) plane preferentially and there is high density of V=O groups in this plane [55,56]. However, as can be seen from Fig. 3, the characteristic peaks due to crystalline V_2O_5 or its dispersed form are totally absent. Thus, vanadia does not form a layer structure on the CaO–TiO$_2$ surface like on various other single oxide supports and stabilized by interaction with the support surface and present in a form that is not detectable as bulk V_2O_5 [1,17,44].

Raman spectra of CaO–TiO$_2$ and 10 wt.% V_2O_5/CaO–TiO$_2$ samples calcined at 723 K are shown in Fig. 4. The Raman bands pertaining to TiO$_2$-anatase phase appear at 147, 196, 397, 514, and 638 cm^{-1} [57]. Also prominent bands pertaining to CaCO$_3$ ($\sim$1080 and 284 cm^{-1}) are noted in line with XRD observations. Both the samples show the typical characteristic Raman bands due to titania-anatase phase. On increase of calcination temperature from 723 to 1073 K, an increase in the intensity of the Raman bands due to titania-anatase phase are noted. No characteristic bands due to TiO$_2$-rutile, CaO or Ca–Ti oxides were observed. As per literature reports, crystalline vanadia shows characteristic features at around 146, 284, 404, 527, 702, and 995 cm^{-1} [4]. Due to a relatively large Raman scattering cross section of V_2O_5 as compared to the cross section of supported vanadia species, Raman spectra of supported vanadia catalysts can appear to be essentially similar to that of bulk V_2O_5 [1]. As shown in Fig. 4, no Raman bands due to crystalline or dis-
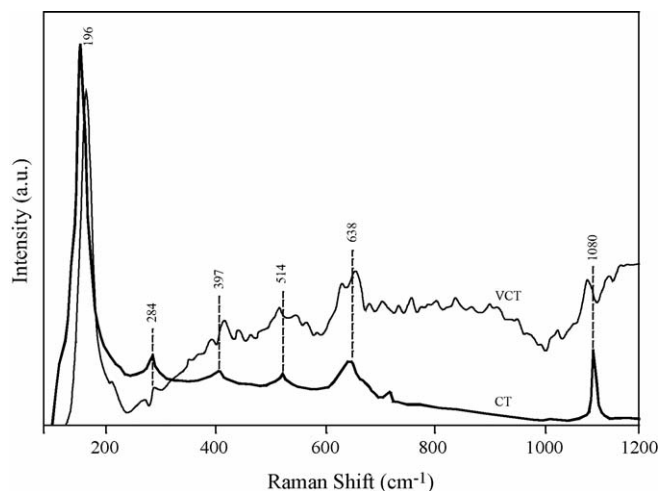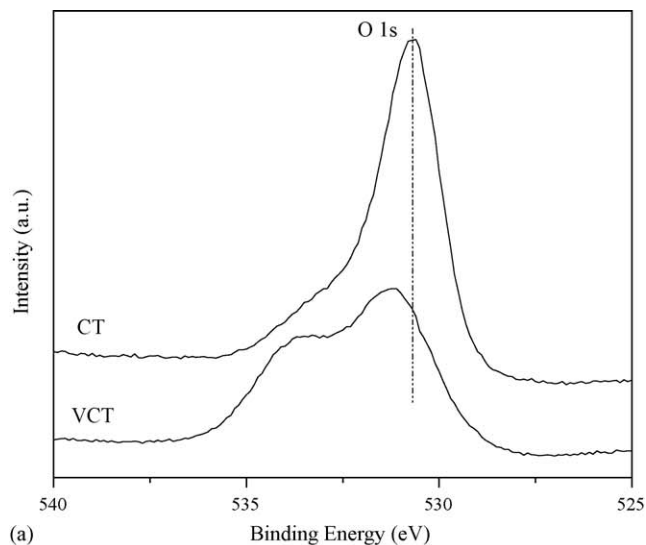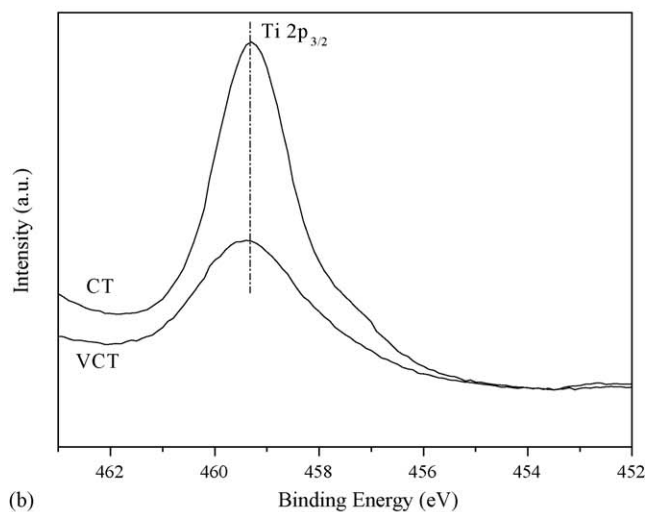
Fig. 4. Raman spectra of CaO–TiO$_2$ (CT) and 10 wt.% V$_2$O$_5$/CaO–TiO$_2$ (VCT) samples calcined at 723 K.

persed vanadia phase are observed. These findings corroborate well with the observations made from XRD and FTIR studies.

To investigate interaction between the supported oxide and the supporting oxide, XPS is a versatile technique. The photoelectron peaks of O 1s, Ti 2p, and Ca 2p pertaining to CaO–TiO$_2$ and 10 wt.% V$_2$O$_5$/CaO–TiO$_2$ samples calcined at 723 K are presented in Fig. 5a–c, respectively. It can be understood from this figure that the photoelectron peaks are sensitive to the coverage of the vanadia on the CaO–TiO$_2$ composite oxide support. The O 1s profile is broad and complicated due to overlapping contribution of oxygen from calcia and titania in the case of CaO–TiO$_2$ and calcia, titania and vanadia in the case of V$_2$O$_5$/CaO–TiO$_2$ sample, respectively. This influence is more prominent in the case of V$_2$O$_5$/CaO–TiO$_2$ sample, which is composed of more than one distinct peak (Fig. 5a). The peak at lower binding energy range is due to the O atoms that are bound to Ti and the peak at higher binding energy could be assigned to Ca as per the literature reports [52,58]. The binding energy of the Ti 2p$_{3/2}$ photoelectron peak (Fig. 5b) ranged between 458.5–459.3 eV, which agrees well with the literature [52,58]. As in the case of O 1s profile, the Ti 2p peak of V$_2$O$_5$/CaO–TiO$_2$ sample also broadened with increase of calcination temperature due to redistribution of various components in the sample (not shown). The redistribution phenomenon is expected because of strong interaction between the acidic V$_2$O$_5$ and the basic CaO to form the stable CaVO$_3$ compound. The Ca 2p photoelectron peaks of the samples (Fig. 5c) also exhibit broad features typical of calcium oxide inline with literature reports [47,48]. A small increase in the binding energy is noticed in the case of V$_2$O$_5$/CaO–TiO$_2$ sample. The intensity of the Ca 2p lines is observed to be almost independent of the calcination temperature in case of CaO–TiO$_2$ sample (spectra not shown), which confer the same chemical state of Ca in the support. In contrast, for V$_2$O$_5$/CaO–TiO$_2$ sample, increase in Ca 2p binding energy as well as peak intensity is noted with increasing calcination temperature. This could be due to the compound formation between CaO and titania or vanadia as stated earlier. The V 2p photoelectron peaks of V$_2$O$_5$/CaO–TiO$_2$ samples are very
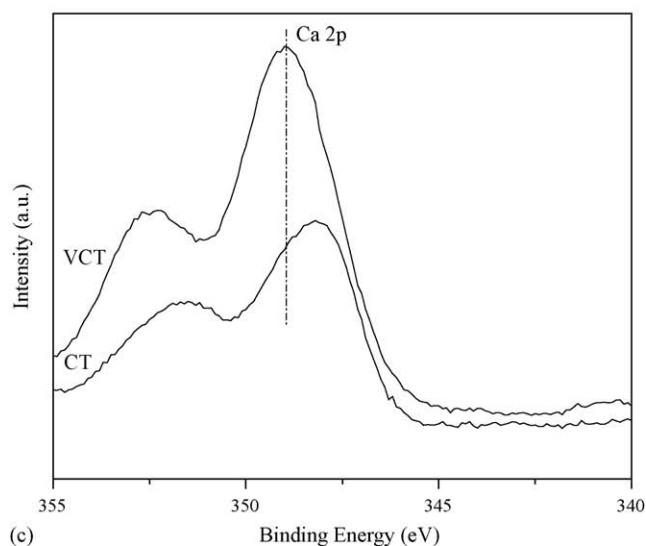
Fig. 5. (a) O 1s, (b) Ti 2p, and (c) Ca 2p XPS spectra of the CaO–TiO$_2$ (CT) and 10 wt.% V$_2$O$_5$/CaO–TiO$_2$ (VCT) samples calcined at 723 K.

broad and less in intensity due to presence of more than one type of V^{5+} or V^{4+} species with different chemical characteristics and electron transfer between the active component and the supporting oxides [58]. As noted from XRD analysis the formation of $CaVO_3$ also contributes to the broadening of the V 2p peak and lowering of its biding energy from its normal V^{5+} oxidation state [52,58]. It is a well-established fact in the literature that V_2O_5 on TiO_2 support accelerates the phase transformation from anatase to rutile and during this transformation some of the dispersed vanadium oxide is reduced and gets incorporated into the rutile structure as $V_xTi_{1-x}O_2$ [1,52]. The results in the present investigation reveal that a strong interaction between CaO and dispersed V_2O_5 inhibits the formation of rutile solid solution and leads to the formation of $CaVO_3$ at higher calcination temperatures. Thus the incorporated CaO to TiO_2 acts as titania-anatase phase stabilizer indirectly.

The steady state activity and selectivity results of cyclohexanol conversion over CaO–TiO_2, 5% V_2O_5/CaO–TiO_2 and 10% V_2O_5/CaO–TiO_2 catalysts (723 K calcined) investigated between 623 and 723 K under normal atmospheric pressure are presented in Fig. 6a–c, respectively. In general the conversion of cyclohexanol increased with increasing reaction temperature irrespective of the catalyst used. However, the product selectivity distribution varied depending on the nature of the catalyst investigated. As can be noted from Fig. 6a–c that more selectivity towards cyclohexanone is observed over CaO–TiO_2 and cyclohexene over vanadia impregnated CaO–TiO_2 catalysts. Dehydration of cyclohexanol gives cyclohexene while dehydrogenation yields cyclohexanone as the ultimate products. The cyclohexene selectivity is usually related to the surface acidity and the cyclohexanone to surface basicity of the catalysts [59]. In fact, a direct correlation was also reported between Brønsted acid sites and the amount of cyclohexene, the dehydration product, formed. The dehydrogenation product, cyclohexanone, was also correlated directly with the basic sites [45]. Obviously, as per the selectivity results the CaO–TiO_2 surface exhibits more basic character whereas V_2O_5/CaO–TiO_2 possesses more acidic sites. The preparation procedure adopted in the present investigation, where an oxide or hydrous oxide sample is formed by condensation and polymerisation of the hydroxylated metal ions precipitated from an aqueous solution, there is a possibility of formation of coordinatively unsaturated metal cations and oxygen anions on the surface of the resulting composite oxides. It is a well-established fact in the literature that exposed coordinatively unsaturated metal cations and oxygen anions on the surface act as Lewis acid and Brønsted base sites [1,3]. The formation of more amounts of cyclohexanone over the CaO–TiO_2 binary oxide than on the vanadia impregnated samples may presumably be due to the presence of more surface oxygen anions, which are expected to be generated in the preparation stage [44]. It can also be noted that as vanadia is impregnated on the surface of calcia-titania binary oxide, a significant improvement in the selectivity towards cyclohexene occurs. As per the literature report [45], the V_2O_5 is a typical acid, possesses only Brønsted acid sites and produces cyclohexene as the sole product in the reaction of cyclohexanol. The increase in selectivity towards cyclohexene on vanadia impregnated CaO–TiO_2
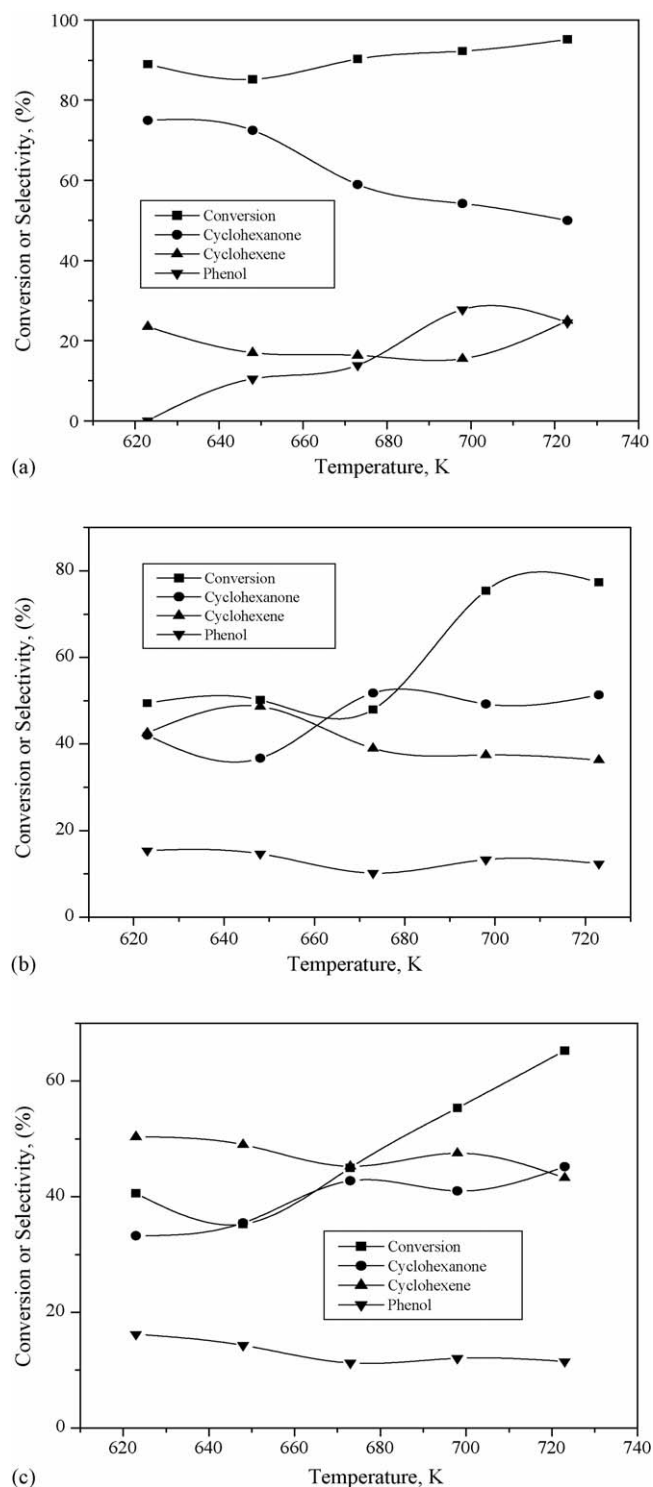

Fig. 6. Activity and selectivity results of cyclohexanol conversion over (a) CaO–TiO_2, (b) 5 wt.% V_2O_5/CaO–TiO_2, and (c) 10 wt.% V_2O_5/CaO–TiO_2 catalysts at various temperatures and under normal atmospheric pressure.

catalyst suggests that vanadia has covered the surface of the support. It can also be stated that vanadium oxide is covering the surface of the CaO–TiO_2 carrier leading to the formation of dispersed vanadium oxide species possessing more surface exposed hydroxyl groups. In other words, with the impregnation of vanadia, the exposed coordinatively unsaturated sites are dras-

tically decreased on the surface and hence significant lowering of the cyclohexanone selectivity is observed. A close observation of Fig. 6 reveals that a higher selectivity for cyclohexanone and cyclohexene over CaO–TiO$_2$ and V$_2$O$_5$/CaO–TiO$_2$ samples, respectively, is observed at lower reaction temperatures. Of course, cyclohexanol conversion increased with increase of reaction temperature as expected. The activity results reveal clearly that vanadia impregnated calcia–titania contains more acidic sites on the surface than that of pure support.

4. Conclusions

The following conclusions can be drawn from this systematic investigation: (1) the incorporated CaO to TiO$_2$ acts as an effective additive for titania-anatase phase stabilization. The CaO–TiO$_2$ mixed oxide contains mainly anatase phase and at higher calcination temperatures some portions of this mixed oxide is converted into CaTiO$_3$ and is thermally quite stable up to 1273 K. (2) The CaO–TiO$_2$ binary oxide is a promising support for V$_2$O$_5$ dispersion. Impregnated V$_2$O$_5$ remains in a highly dispersed and amorphous state over the support and the dispersion behaviour is dependent upon the vanadia loading. (3) In particular, the formation of CaVO$_3$ compound in the case of V$_2$O$_5$/CaO–TiO$_2$ samples as inferred by XRD and XPS observations, inhibits the formation of the most feasible V$_x$Ti$_{(1-x)}$O$_2$ (rutile solid solution) at higher calcination temperatures. (4) The CaO–TiO$_2$ mixed oxide exhibits more cyclohexanone selectivity and V$_2$O$_5$/CaO–TiO$_2$ more cyclohexene selectivity in the conversion of cyclohexanol reflecting their basic and acidic properties, respectively. Further work is under active progress to exploit these catalysts for commercially important reactions.

References

[1] G.C. Bond, S.F. Tahir, Appl. Catal. 71 (1991) 1, and references therein.
[2] G. Deo, I.E. Wachs, J. Haber, Crit. Rev. Surf. Chem. 4 (1994) 141.
[3] D.J. Hucknall, Selective Oxidation of Hydrocarbons, Academic Press, London, 1974.
[4] B.M. Reddy, P. Lakshmanan, A. Khan, J. Phys. Chem. B 108 (2004) 16855.
[5] E.P. Reddy, R.S. Varma, J. Catal. 221 (2004) 93.
[6] I.E. Wachs, R.Y. Saleh, S.S. Chan, C.C. Cherich, Appl. Catal. 77 (1982) 309.
[7] P. Cavalli, F. Cavani, I. Manenti, F. Trifiro, Catal. Today 1 (1987) 245.
[8] B.M. Reddy, B. Manohar, Chem. Ind. (London) (1992) 182.
[9] H. Bosch, F. Janssen, Catal. Today 2 (1988) 369 and references therein.
[10] J.N. Armor (Ed.), ACS Symposium Series, vol. 552, American Chemical Society, Washington, DC, 1994.
[11] I.E. Wachs, G. Deo, B.M. Weckhuysen, A. Andreini, M.A. Vuurman, M. de Boer, M.D. Amiridis, J. Catal. 161 (1996) 211.
[12] J. Armor, Appl. Catal. B 1 (1992) 221.
[13] J.P. Dunn, P.R. Koppula, H.G. Stenger, I.E. Wachs, Appl. Catal. B 19 (1998) 103.
[14] K. Chen, A. Khodakov, J. Yang, A.T. Bell, E. Iglesia, J. Catal. 186 (1999) 325.
[15] P. Concepcion, J.M. Lopez-Nieto, J. Perez-Pariente, J. Mol. Catal. A: Chem. 97 (1995) 173.
[16] J.C. Vedrine (Ed.), Catal. Today 20 (1994) 1, and references therein.
[17] B.M. Reddy, E.P. Reddy, S.T. Srinivas, V.M. Mastikin, A.V. Nosov, O.B. Lapina, J. Phys. Chem. 96 (1992) 7076.
[18] B.M. Reddy, P.M. Sreekanth, E.P. Reddy, Y. Yamada, Q. Xu, H. Sakurai, T. Kobayashi, J. Phys. Chem. B 106 (2002) 5695.
[19] Z. Sobalic, R. Kozlowski, J. Haber, J. Catal. 127 (1991) 665.
[20] B.E. Handy, M. Maciejewski, A. Baiker, J. Catal. 134 (1992) 75.
[21] H. Zou, M. Li, J. Shen, A. Auroux, J. Therm. Anal. Calorim. 72 (2003) 209.
[22] K.I. Hadjiivanov, D.G. Klissurski, Chem. Soc. Rev. 25 (1996) 61.
[23] M. Anpo, Res. Chem. Intermed. 11 (1989) 67.
[24] M. Taramasso, G. Perego, B. Notari, U.S. Patent 4,410,501 (1983).
[25] P. Cavilli, F. Cavini, I. Manenti, F. Trifiro, Ind. Eng. Chem. Res. 26 (1987) 804.
[26] A.L. Linsebigler, G. Lu, J.T. Yates Jr., Chem. Rev. 95 (1995) 735.
[27] J. Haber, Oxygen in Catalysis, Decker, New York, 1991.
[28] S. Lars, J. Anderson, J. Chem. Soc. Faraday Trans. I 75 (1979) 1359.
[29] A. Anderson, S.T. Lundin, J. Catal. 65 (1980) 9.
[30] G. Deo, I.E. Wachs, J. Catal. 129 (1991) 307.
[31] G. Deo, I.E. Wachs, J. Catal. 146 (1994) 323.
[32] G. Busca, A.S. Elmi, P. Forzatti, J. Phys. Chem. 91 (1987) 5263.
[33] Y.S. Lin, C.H. Chang, R. Gopalan, Ind. Eng. Chem. Res. 33 (1994) 860.
[34] H. Schaper, E.B.M. Doesburg, P.H.M. De Korte, L.L. Van Reijen, Solid State Ionics 16 (1985) 261.
[35] S. Hishita, I. Mutoh, K. Koumoto, H. Yanagida, Ceram. Int. 9 (1983) 61.
[36] K.N.P. Kumar, K. Keizer, A.J. Burggraaf, J. Mater. Sci. Lett. 13 (1994) 59.
[37] J. Cunningham, C. Healy, D. McNamara, S. O'Brien, Catal. Today 2 (1988) 557.
[38] K. Omata, A. Aoki, K. Fujimoto, Catal. Lett. 4 (1990) 241.
[39] C.T. Au, K.D. Chen, C.F. Ng, Appl. Catal. A: Gen. 170 (1998) 81.
[40] J. Kijenski, A. Baiker, Catal. Today 5 (1989) 1.
[41] M. Ai, J. Mol. Catal. A: Chem. 114 (1996) 3.
[42] B.M. Reddy, E.P. Reddy, I. Ganesh, M.V. Kumar, Ind. J. Chem. Technol. 4 (1997) 256.
[43] B.M. Reddy, I. Ganesh, B. Chowdhary, Chem. Lett. (1997) 1145.
[44] B.M. Reddy, I. Ganesh, J. Mol. Catal. A: Chem. 169 (2001) 207.
[45] C.P. Bezouhanova, M.A. Al-Zihari, Catal. Lett. 11 (1991) 245.
[46] S. Jaenicke, Catal. Surveys Asia 9 (3) (2005) 173, and references therein.
[47] D. Briggs, M.P. Seah (Eds.), Practical Surface Analysis, Auger and X-ray Photoelectron Spectroscopy, vol. 1, 2nd ed., Wiley, New York, 1990.
[48] C.D. Wagner, W.M. Riggs, L.E. Davis, J.F. Moulder, in: G.E. Muilenberg (Ed.), Handbook of X-Ray Photoelectron Spectroscopy, Perkin-Elmer Corporation, Minnesota, 1978.
[49] B.M. Reddy, A. Khan, Y. Yamada, T. Kobayashi, S. Loridant, J.C. Volta, J. Phys. Chem. B 107 (2003) 11475.
[50] B.M. Reddy, A. Khan, Y. Yamada, T. Kobayashi, S. Loridant, J.C. Volta, J. Phys. Chem. B 106 (2002) 10964.
[51] B.M. Reddy, B. Manohar, E.P. Reddy, Langmuir 9 (1993) 1781.
[52] B.M. Reddy, I. Ganesh, E.P. Reddy, J. Phys. Chem. B 101 (1997) 1769.
[53] R.A. Nyquist, R.O. Kagel, The Handbook of Infrared and Raman Spectra of Inorganic Compounds and Organic Salts, vol. 4, Academic Press Inc., 1997.
[54] T. Hirata, K. Ishioka, M. Kitajima, J. Solid State Chem. 124 (1996) 353.
[55] A. Miyamoto, Y. Yamazaki, M. Inomata, Y. Murakami, J. Phys. Chem. 85 (1981) 2366.
[56] M. Inomata, A. Miyamoto, Y. Murakami, J. Phys. Chem. 85 (1981) 2372.
[57] X.-M. Lin, L.-P. Li, G.-S. Li, W.-H. Su, Mater. Chem. Phys. 69 (2001) 236.
[58] B.M. Reddy, B. Chowdhary, I. Ganesh, E.P. Reddy, T.C. Rojas, A. Fernandez, J. Phys. Chem. B 102 (1998) 10176.
[59] D. Martin, D. Duprez, J. Mol. Catal. 118 (1997) 113.